Sisyphus Laser Cooling of a Polyatomic Molecule

Ivan Kozyryev,[*] Louis Baum, Kyle Matsuda,[†] Benjamin L. Augenbraun, Loic Anderegg,
Alexander P. Sedlack, and John M. Doyle

[1]*Harvard-MIT Center for Ultracold Atoms, Cambridge, Massachusetts 02138, USA*
[2]*Department of Physics, Harvard University, Cambridge, Massachusetts 02138, USA*
(Received 20 September 2016; published 24 April 2017)

We perform magnetically assisted Sisyphus laser cooling of the triatomic free radical strontium monohydroxide (SrOH). This is achieved with principal optical cycling in the rotationally closed $P(N'' = 1)$ branch of either the $\tilde{X}^2\Sigma^+(000) \leftrightarrow \tilde{A}^2\Pi_{1/2}(000)$ or the $\tilde{X}^2\Sigma^+(000) \leftrightarrow \tilde{B}^2\Sigma^+(000)$ vibronic transitions. Molecules lost into the excited vibrational states during the cooling process are repumped back through the $\tilde{B}(000)$ state for both the (100) level of the Sr-O stretching mode and the (02^00) level of the bending mode. The transverse temperature of a SrOH molecular beam is reduced in one dimension by 2 orders of magnitude to $\sim750\ \mu$K. This approach opens a path towards creating a variety of ultracold polyatomic molecules by means of direct laser cooling.

Compared to atoms, the additional rotational and vibrational degrees of freedom in molecules give rise to a wide variety of potential and implemented scientific applications, including quantum computation [1–3], precision measurements [4–7], and quantum simulation [8,9]. While ultracold diatomic molecules will be valuable in opening novel research frontiers, molecules with three or more atoms have unique capabilities for advancing fundamental physics [10–12], chemistry [13,14], and quantum technologies [15–17]. Cooling molecular degrees of freedom significantly aids in realizing such applications. Yet, the desired quantum complexity that molecules provide also leads to challenges for control, detection, and cooling [18]. Assembling ultracold molecules from two laser-cooled atoms has represented one solution and created ultracold bi-alkali molecules [19–23], including filling of optical lattices [24,25]. Direct cooling techniques routinely cool a much wider variety of molecules into the Kelvin regime [18,26]. Intense research is ongoing to bring these cold molecules into the ultracold regime (< 1 mK). Even though there has been experimental progress on control of polyatomics [27–32], optoelectrical cooling of formaldehyde is the only technique that has resulted in a trapped submillikelvin sample [33].

Cooling of the external motion of neutral atoms from above room temperature into the submillikelvin range (leading to, e.g., Bose-Einstein condensation) commonly relies on the use of velocity-dependent optical forces [34]. Laser cooling requires reasonably closed and strong optical electronic transitions, so its use for molecules has been severely limited. Recently, following initial theoretical proposals [35,36] and proof-of-principle experimental results [37], laser cooling has been achieved for SrF [38], YO [39], and CaF [40,41], including a magneto-optical trap (MOT) for SrF [42–44]. Motivated by this

progress on diatomic molecules, and building upon previous theoretical work [45], we recently demonstrated photon cycling—a crucial requirement for achieving light induced forces—with the triatomic molecule SrOH [46]. However, since SrOH had 3 distinct vibrational modes, including a doubly degenerate bending mode, and because Doppler cooling required scattering an order of magnitude more photons as compared to deflection experiments, the question of direct laser cooling remained open.

In this Letter, we report efficient Sisyphus laser cooling of a polyatomic molecule from 50 mK to below 1 mK in 1 dimension. The dissipative force for compressing phase space volume is achieved by a combination of spatially varying light shifts and optical pumping into dark sublevels, which are then remixed by a static magnetic field, as explored previously in atomic systems [47,48]. Since the magnitude of the induced friction force is directly related to the modulation depth of the dressed energy levels, the cooling process is much more efficient than with Doppler radiation pressure forces [49,50]. This enhancement is especially important for complex polyatomic molecules, where scattering the thousands of photons necessary for Doppler cooling becomes more challenging due to additional vibrational modes [51]. Here, we demonstrate transverse cooling (and heating) of a SrOH beam using two different electronic transitions, study loss channels to excited vibrational states (including the bending mode), and highlight proposed extensions to more complex strontium monoalkoxides with six and more atoms.

Our work with SrOH uses the cryogenic buffer-gas beam (CBGB) [52], which is also used in all other experiments on laser cooling of molecules. The study of SrOH buffer-gas cooling dynamics, as well as precise measurements of its momentum transfer and inelastic cross sections with helium, were previously performed [53]. In brief, SrOH

can be produced efficiently with ablation and forms an intense CBGB. Figure 1(a) shows a simplified schematic diagram of the current experimental apparatus. Detailed descriptions of this apparatus have also been provided elsewhere [56]. Laser ablation of $Sr(OH)_2$ produces SrOH molecules that are then entrained in helium buffer gas ($T_{He} \sim 2$ K) that flows out of the cell into a beam. He flow is 6 standard cubic centimeters per minute (sccm), and the beam is extracted through a 5 mm diam aperture. This CBGB contains $\sim 10^9$ molecules in the first excited rotational level ($N = 1$) in a pulse ~ 5 ms long. The forward velocity of the SrOH beam is $v_x \sim 130$ m/s and its transverse velocity spread is $\Delta v_y \sim \pm 15$ m/s. A 2×2 mm square aperture situated 15 cm away from the cell collimates the beam, resulting in an effective transverse temperature $T_\perp \sim 50$ mK. A few millimeters after the aperture, molecules enter the interaction region with molecule-laser interaction length of 15 mm.

To laser cool, we use a photon cycling scheme that we also employed in an earlier work, as described in detail in Ref. [46]. The main photon cycling path is $\tilde{X}^2\Sigma^+(000) \rightarrow \tilde{B}^2\Sigma^+(000)$ (611 nm) and the first vibrational repump is $\tilde{X}^2\Sigma^+(100) \rightarrow \tilde{B}^2\Sigma^+(000)$ (631 nm), as shown in Fig. 1(a)

(interaction region). The combined main and repump laser light, with diameter of ~ 3 mm, propagates in the y direction and makes 5 round-trip passes between two mirrors before it is retroreflected back in order to create a standing wave. The molecule-laser interaction time is $t_{int} \sim 115$ μs. Each color (611 and 631 nm) includes two frequency components separated by ~ 110 MHz to address the $P_{11}(J'' = 1.5)$ and $^PQ_{12}(J'' = 0.5)$ lines of the spin-rotation (SR) splitting [Fig. 1(b)]. We also study cooling using the $\tilde{X}^2\Sigma^+(000) \rightarrow \tilde{A}^2\Pi_{1/2}(000)$ excitation at 688 nm as the main transition. Each SR component of the 688 nm light is generated using separate injection-locked laser diodes seeded by external-cavity diode lasers in the Littrow configuration [57] resulting in ~ 15 mW per SR component in the interaction region. The 611 nm light, as well as all of the repumping light, is generated by cw dye lasers passing through acousto-optic modulators resulting in ~ 50 mW per SR component. In order to destabilize dark states created during the cycling process [58], we apply a magnetic field of a few gauss. Because of the vibrational angular momentum selection rule [59], the dominant loss channel for the bending mode is to the $v_2 = 2$ state with $l = 0$ [60] denoted (02^00). Further details regarding the
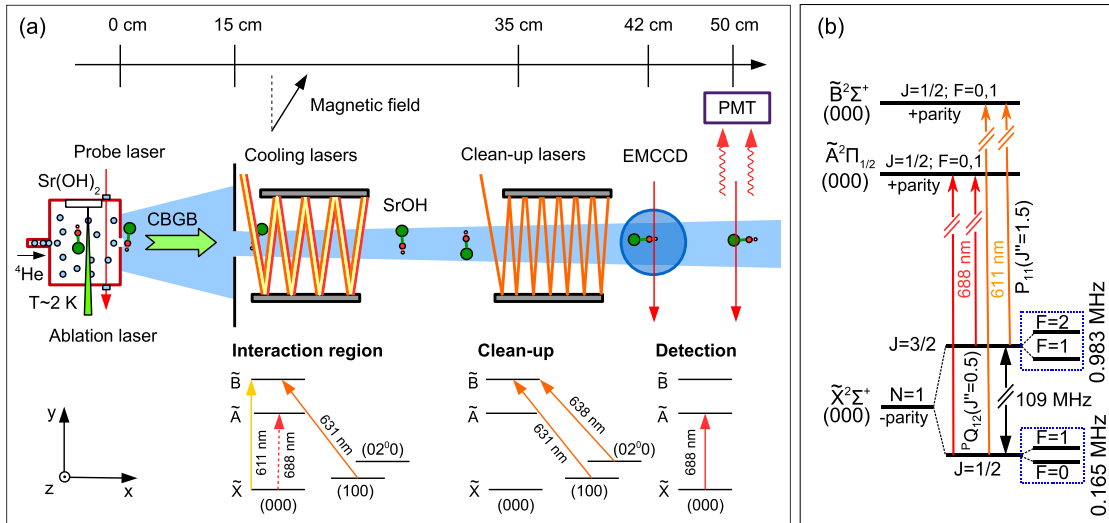

FIG. 1. (a) Schematic of the experimental apparatus (not to scale). A cryogenic beam of SrOH is produced using laser ablation of $Sr(OH)_2$ followed by buffer-gas cooling with ~ 2 K helium gas. To apply the cooling forces on the collimated molecular beam, we use transverse lasers retroreflected between two mirrors in order to generate a standing wave. Depending on the experimental configuration, either the $\tilde{X}^2\Sigma^+(000) \rightarrow \tilde{A}^2\Pi_{1/2}(000)$ or the $\tilde{X}^2\Sigma^+(000) \rightarrow \tilde{B}^2\Sigma^+(000)$ cooling transition is used with an additional $\tilde{X}^2\Sigma^+(100) \rightarrow \tilde{B}^2\Sigma^+(000)$ laser for repumping molecules decaying to the vibrationally excited Sr-O stretching mode. In order to remix dark magnetic sublevels, a magnetic field is applied at an angle relative to laser polarization in the interaction region. Before the detection is performed, molecules remaining in either the (100) or (02^00) excited vibrational levels of the electronic ground state are optically pumped back into the ground vibrational level using $\tilde{X} \rightarrow \tilde{B}$ off-diagonal excitations. The spatial profile of the molecular beam is imaged on the electron multiplying charge-coupled device (EMCCD) camera and the time of flight data are collected on the photomultiplier tube (PMT). The vibrational quantum numbers $(v_1 v_2^l v_3)$ correspond to the Sr $\leftrightarrow$ OH stretching (v_1), Sr-O-H bending (v_2), and SrO $\leftrightarrow$ H stretching (v_3) vibrational modes. The superscript l next to the bending mode vibrational quantum number indicates the projection of the vibrational angular momentum on the internuclear axis. (b) Relevant rotational, fine, and hyperfine structure of SrOH. Rotationally closed excitations on the $\tilde{X} - \tilde{A}$ and $\tilde{X} - \tilde{B}$ electronic transition are shown with red and orange upward arrows, correspondingly. The unresolved hyperfine splittings have been previously measured [54] and are smaller than the natural linewidth of the electronic transitions [55].
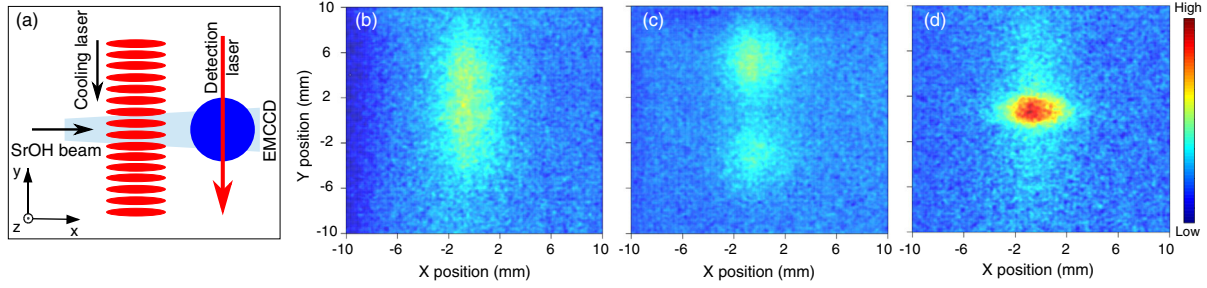
FIG. 2.   Spatial images of the molecular beam taken at different detunings of the $\tilde{X}(000) - \tilde{B}(000)$ cooling laser: (b) on resonance, (c) red-detuned (-10 MHz), and (d) blue-detuned ($+10$ MHz). SrOH beam is moving in the x direction while the cooling and detection lasers are applied in the y direction as shown in (a). Narrowing of the spatial size of the molecular cloud with accompanying density increase in (d) compared to (b) in the y dimension indicates phase space compression.

photon cycling scheme used for SrOH have been previously described [46].

The spatial profile of the molecular beam is recorded by imaging laser-induced fluorescence (LIF) in the detection region. The molecules are excited using a transverse retroreflected laser beam and LIF photons are imaged onto an EMCCD camera. The detection laser addresses both SR components of the $P(N'' = 1)$ line for the $\tilde{X}^2\Sigma^+(000) \rightarrow \tilde{A}^2\Pi_{1/2}(000)$ transition, as shown in Fig. 1(a) (detection). In a similar laser configuration, time of flight (TOF) data are recorded by collecting the LIF on a PMT (further downstream). In order to boost the LIF signal there is a clean-up region where all of the molecular population is pumped into the ground state [$\tilde{X}(000)$] from the excited vibrational levels [$\tilde{X}(100)$ and $\tilde{X}(02^0 0)$]. This is done with off-diagonal excitation to $\tilde{B}(000)$, as shown in Fig. 1(a) (clean-up).

Figure 2 shows 2D camera images of the molecular beam for various detunings of the $\tilde{X} - \tilde{B}$ cooling laser. Phase

space compression is clearly visible in the comparison between images (b) $\delta = 0$, and (d) $\delta > 0$, cooling. To characterize the cooling efficacy for both $\tilde{X} - \tilde{A}$ and $\tilde{X} - \tilde{B}$ cycling transitions, we plot integrated 1D (x axis) beam profiles for both cooling configurations in Fig. 3. The most effective laser cooling was demonstrated using $\tilde{X}(000) - \tilde{B}(000)$ transition at 611 nm with laser intensity $I = 1.4$ W/cm^2, resulting in a saturation parameter $s \sim 34$ [Fig. 3(a)]. The spatial distribution of the final beam is the convolution of the initial 2×2 mm beam spread, the beam spread before cooling, and the beam spread after cooling. Without cooling, the spatial width of the molecular beam is dominated by the transverse velocity distribution $v_\perp$ after the collimation aperture. In the Sisyphus configuration, the spatial profile in the detection region is influenced by the aperture's width. In order to extract $v_\perp$, Monte Carlo (MC) simulations of 2D molecular trajectories are performed by calculating the final y position in the detection region of the molecules with forward
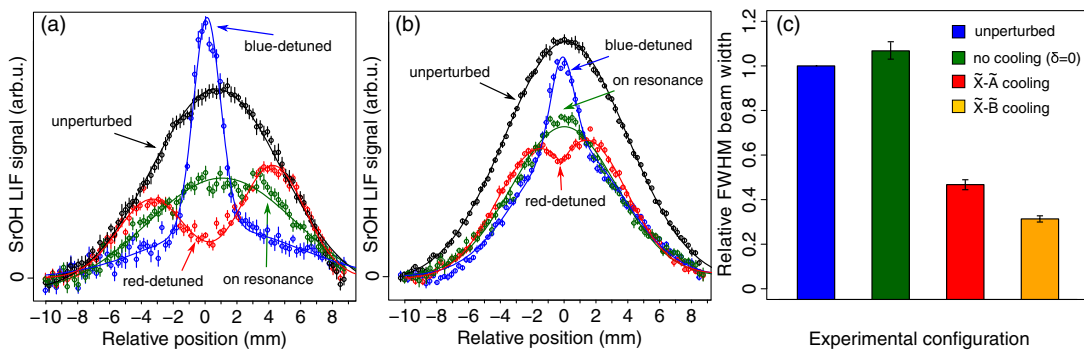

FIG. 3.   Integrated molecular beam profiles for different detunings of the cooling laser: (a) $\tilde{X}(000) - \tilde{B}(000)$ and (b) $\tilde{X}(000) - \tilde{A}(000)$. The detunings from resonance are given by $\delta = \pm 10$ MHz. With a positive detuning, the width of the molecular beam is reduced, which indicates cooling of the molecular beam. A "hole" around zero for $\delta < 0$ represents a heating signature of the magnetically assisted Sisyphus effect with the widening of the total spatial distribution. An asymmetry in the height of two peaks comes from imperfect alignment between laser and molecular beams and was previously seen in similar experiments with atoms [49]. The excess signal above the fit near zero position for the on-resonance trace in (b) is potentially indicative of a slightly positive detuning of the cooling lasers. (c) Summary of the cooling results in terms of the FWHM of the molecular cloud in the y dimension relative to the unperturbed distribution (no cooling lasers). Without cooling ($\delta = 0$) the molecular beam profile is not modified significantly.

velocity v_x that passed through the collimation aperture. The molecular velocities in the y direction are drawn from a Gaussian distribution with a standard deviation $\sigma_{v_y} = \sqrt{k_B T_\perp / m}$, where m is the mass of SrOH. By fitting the results of the MC simulations to the integrated molecular beam profiles, we determine the final beam temperature range of 0.5 mK $< T_\perp <$ 1 mK, which corresponds to a factor of $\sim$70 reduction as compared to the $\delta = 0$ detuning and unperturbed molecular beam. Because of the high damping rate of the magnetic-field-induced laser cooling [48,61], we achieve lower transverse temperature than previously demonstrated with a 1D MOT of diatomic molecules [39], with half the interaction length.

Cooling using the $\tilde{X} - \tilde{A}$ transition was less effective. Figure 3(b) shows typical molecular beam profiles after interacting with a cooling laser exciting the $\tilde{X} - \tilde{A}$ transition at 688 nm with intensity of $I = 424$ mW/cm^2 and a saturation parameter $s \sim 8$. For a positive detuning, we observe cooling of the SrOH beam represented by the increased molecular density near the center due to the narrowing of the spatial distribution. By comparing the fitted width of the resulting profile with a MC simulation, we conclude that the beam is cooled to a final temperature of $\sim$2 mK, an order of magnitude above the Doppler limit of $\sim$200 μK. Figure 3(c) summarizes the cooling data for all configurations by plotting the full width at half maximum (FWHM) in the y dimension of the imaged molecular beam relative to the width of the unperturbed beam. While for the on-resonance configuration of the cooling lasers the width of the beam is not significantly modified, blue-detuned $\tilde{X} - \tilde{A}$ and $\tilde{X} - \tilde{B}$ lasers compress molecular beam to 47% and 31% of the original FWHM.

Figures 3(a) and 3(b) show that during the cooling process 40% of the molecules are lost to dark excited vibrational levels not addressed by the (100) and (02^{0}0) repumping lasers. The phase space density Ω [62] of the molecular beam is increased due to cooling, with temperature reduction and spatial beam compression. The peak on-axis Ω [63] grows $\times$5 with $\tilde{X} - \tilde{A}$ and $\times$11 with $\tilde{X} - \tilde{B}$ cooling. With the two repumping lasers used in the experiment, $\sim$10^6 molecules remain in the $N = 1$ (000) level. Lost molecules could be recovered with an additional repumping laser addressing the (200) vibrational level of the Sr-O stretching mode.

In order to extract the number of scattered photons during the cooling process, we determine the fraction of the remaining molecules (50%) after cooling with TOF PMT data taken without the (02^{0}0) clean-up beam. Modeling absorption-emission cycles as a Bernoulli process with probability p to decay into the vibrational level not addressed by the repumping lasers [35] and using the previously measured decay rate to dark vibrational levels [above $\tilde{X}$(100)] of $p = (3 \pm 1) \times 10^{-3}$ [46], we calculate

that on average each molecule emits 220$^{+110}_{-60}$ photons with a scattering rate of $\Gamma_{\text{scat}} = 2 \pm 1$ MHz. In such a configuration, Doppler cooling from radiation-pressure molasses does not play a significant role [49]. By adding the (02^{0}0) clean-up beam, we determine that 10% of molecules decay to the (02^{0}0) state of the bending mode during the cooling stage.

For negative detunings, the molecules are expelled from the region around $v_y = 0$, leading to a double-peak structure that is a signature of the magnetically assisted Sisyphus effect [47]. Compared to the results of cycling on the $\tilde{X} - \tilde{A}$ transition [Fig. 3(b)], the use of the $\tilde{X} - \tilde{B}$ transition [Fig. 3(a)] increases the separation between the peaks from 2.95 $\pm$ 0.04 to 7.54 $\pm$ 0.04 mm for $\delta < 0$. Our findings are in good agreement with previous studies of sub-Doppler laser cooling in complex multilevel atomic [64] and molecular systems [38,65].

In summary, we demonstrate Sisyphus laser cooling of the polyatomic molecule SrOH. We reduce the transverse temperature of a cryogenic buffer-gas beam from 50 mK to 750 μK with $\sim$200 scattered photons per molecule. Laser cooling of atoms is a mature scientific field [66–68] with well-developed experimental [69,70] and theoretical [71,72] techniques. Our results with SrOH open up a wide range of future directions for laser manipulation of polyatomic molecules. By increasing the interaction time and reducing laser intensity, cooling SrOH to significantly lower temperatures should be possible, as previously demonstrated for atomic species under similar experimental conditions [73,74]. Extending the scheme to two dimensions and using more elaborate optical configurations could lead to significantly increased brightening of the molecular beam [74,75]. Slowing and cooling of an atomic beam in the longitudinal dimension [76,77], e.g., for loading into a MOT, could now be extended to polyatomic molecules.

While some of these research avenues might require repumping of other vibrational states beyond the (100) and (02^{0}0) states as the number of scattered photons increases, this challenge can be solved with additional repumping lasers on the $\tilde{X} - \tilde{B}$ transition. Since the strengths of higher-order Franck-Condon factors decrease rapidly [60,78], scattering of $\sim$10 000 photons should be possible with two additional lasers addressing the (200) and (01^{1}0) states. Moreover, by using $\tilde{X} - \tilde{A}$ electronic excitation for laser cooling and $\tilde{X} - \tilde{B}$ excitation for repumping, the scattering rate becomes independent of the number of repumping lasers, ensuring rapid optical cycling.

While SrOH has a linear geometry in the vibronic ground state, it serves as a useful test candidate for the feasibility of laser cooling more complex, nonlinear molecules like strontium monoalkoxide free radicals, where hydrogen is replaced by a more complex group R (e.g., $R = $ CH$_3$, CH$_2$CH$_3$). Because of the 180° Sr-O-C bond angle, the local symmetry near the optically active electron located

on the strontium atom is linear (like in SrOH). Furthermore, SrOR molecules share a number of other important properties with SrOH, including a very ionic Sr-O bond, diagonal Franck-Condon factors, and technically accessible laser transitions [79,80], indicating feasible extension to such complex species [81].

---

[*] ivan@cua.harvard.edu

[†] Present address: JILA, National Institute of Standards and Technology and University of Colorado, and Department of Physics, University of Colorado, Boulder, CO 80309, USA.

[1] D. DeMille, Phys. Rev. Lett. **88**, 067901 (2002).

[2] P. Rabl, D. DeMille, J. M. Doyle, M. D. Lukin, R. J. Schoelkopf, and P. Zoller, Phys. Rev. Lett. **97**, 033003 (2006).

[3] A. André, D. DeMille, J. M. Doyle, M. D. Lukin, S. E. Maxwell, P. Rabl, R. J. Schoelkopf, and P. Zoller, Nat. Phys. **2**, 636 (2006).

[4] ACME Collaboration, Science **343**, 269 (2014).

[5] R. C. Hilborn and C. L. Yuca, Phys. Rev. Lett. **76**, 2844 (1996).

[6] D. DeMille, Phys. Today **68**, 34 (2015).

[7] D. DeMille, S. B. Cahn, D. Murphree, D. A. Rahmlow, and M. G. Kozlov, Phys. Rev. Lett. **100**, 023003 (2008).

[8] A. Micheli, G. Brennen, and P. Zoller, Nat. Phys. **2**, 341 (2006).

[9] S. R. Manmana, E. M. Stoudenmire, K. R. A. Hazzard, A. M. Rey, and A. V. Gorshkov, Phys. Rev. B **87**, 081106 (2013).

[10] P. Cancio Pastor, I. Galli, G. Giusfredi, D. Mazzotti, and P. De Natale, Phys. Rev. A **92**, 063820 (2015).

[11] M. G. Kozlov, Phys. Rev. A **87**, 032104 (2013).

[12] A. Shelkovnikov, R. J. Butcher, C. Chardonnet, and A. Amy-Klein, Phys. Rev. Lett. **100**, 150801 (2008).

[13] M. Quack, Angew. Chem., Int. Ed. Engl. **41**, 4618 (2002).

[14] M. Quack, J. Stohner, and M. Willeke, Annu. Rev. Phys. Chem. **59**, 741 (2008).

[15] M. Wall, K. Maeda, and L. D. Carr, New J. Phys. **17**, 025001 (2015).

[16] M. L. Wall, K. Maeda, and L. D. Carr, Ann. Phys. (Berlin) **525**, 845 (2013).

[17] C. M. Tesch and R. de Vivie-Riedle, Phys. Rev. Lett. **89**, 157901 (2002).

[18] L. D. Carr, D. DeMille, R. V. Krems, and J. Ye, New J. Phys. **11**, 055049 (2009).

[19] K.-K. Ni, S. Ospelkaus, M. De Miranda, A. Pe'er, B. Neyenhuis, J. Zirbel, S. Kotochigova, P. Julienne, D. Jin, and J. Ye, Science **322**, 231 (2008).

[20] J. W. Park, S. A. Will, and M. W. Zwierlein, Phys. Rev. Lett. **114**, 205302 (2015).

[21] T. Takekoshi, L. Reichsöllner, A. Schindewolf, J. M. Hutson, C. R. Le Sueur, O. Dulieu, F. Ferlaino, R. Grimm, and H.-C. Nägerl, Phys. Rev. Lett. **113**, 205301 (2014).

[22] P. K. Molony, P. D. Gregory, Z. Ji, B. Lu, M. P. Köppinger, C. R. Le Sueur, C. L. Blackley, J. M. Hutson, and S. L. Cornish, Phys. Rev. Lett. **113**, 255301 (2014).

[23] M. Guo, B. Zhu, B. Lu, X. Ye, F. Wang, R. Vexiau, N. Bouloufa-Maafa, G. Quéméner, O. Dulieu, and D. Wang, Phys. Rev. Lett. **116**, 205303 (2016).

[24] S. A. Moses, J. P. Covey, M. T. Miecnikowski, B. Yan, B. Gadway, J. Ye, and D. S. Jin, Science **350**, 659 (2015).

[25] L. Reichsöllner, A. Schindewolf, T. Takekoshi, R. Grimm, and H.-C. Nägerl, Phys. Rev. Lett. **118**, 073201 (2017).

[26] M. Lemeshko, R. V. Krems, J. M. Doyle, and S. Kais, Mol. Phys. **111**, 1648 (2013).

[27] M. Zeppenfeld, B. G. Englert, R. Glöckner, A. Prehn, M. Mielenz, C. Sommer, L. D. van Buuren, M. Motsch, and G. Rempe, Nature (London) **491**, 570 (2012).

[28] S. Chervenkov, X. Wu, J. Bayerl, A. Rohlfes, T. Gantner, M. Zeppenfeld, and G. Rempe, Phys. Rev. Lett. **112**, 013001 (2014).

[29] H. L. Bethlem, G. Berden, F. M. Crompvoets, R. T. Jongma, A. J. Van Roij, and G. Meijer, Nature (London) **406**, 491 (2000).

[30] D. Patterson and J. M. Doyle, Phys. Chem. Chem. Phys. **17**, 5372 (2015).

[31] T. Momose, Y. Liu, S. Zhou, P. Djuricanin, and D. Carty, Phys. Chem. Chem. Phys. **15**, 1772 (2013).

[32] R. Fulton, A. I. Bishop, and P. F. Barker, Phys. Rev. Lett. **93**, 243004 (2004).

[33] A. Prehn, M. Ibrügger, R. Glöckner, G. Rempe, and M. Zeppenfeld, Phys. Rev. Lett. **116**, 063005 (2016).

[34] C. Adams and E. Riis, Prog. Quantum Electron. **21**, 1 (1997).

[35] M. Di Rosa, Eur. Phys. J. D **31**, 395 (2004).

[36] B. K. Stuhl, B. C. Sawyer, D. Wang, and J. Ye, Phys. Rev. Lett. **101**, 243002 (2008).

[37] E. S. Shuman, J. F. Barry, D. R. Glenn, and D. DeMille, Phys. Rev. Lett. **103**, 223001 (2009).

[38] E. S. Shuman, J. F. Barry, and D. DeMille, Nature (London) **467**, 820 (2010).

[39] M. T. Hummon, M. Yeo, B. K. Stuhl, A. L. Collopy, Y. Xia, and J. Ye, Phys. Rev. Lett. **110**, 143001 (2013).

[40] V. Zhelyazkova, A. Cournol, T. E. Wall, A. Matsushima, J. J. Hudson, E. A. Hinds, M. R. Tarbutt, and B. E. Sauer, Phys. Rev. A **89**, 053416 (2014).

[41] B. Hemmerling, E. Chae, A. Ravi, L. Anderegg, G. K. Drayna, N. R. Hutzler, A. L. Collopy, J. Ye, W. Ketterle, and J. M. Doyle, J. Phys. B **49**, 174001 (2016).

[42] J. Barry, D. McCarron, E. Norrgard, M. Steinecker, and D. DeMille, Nature (London) **512**, 286 (2014).

[43] D. McCarron, E. Norrgard, M. Steinecker, and D. DeMille, New J. Phys. **17**, 035014 (2015).

[44] E. B. Norrgard, D. J. McCarron, M. H. Steinecker, M. R. Tarbutt, and D. DeMille, Phys. Rev. Lett. **116**, 063004 (2016).

[45] T. A. Isaev and R. Berger, Phys. Rev. Lett. **116**, 063006 (2016).

[46] I. Kozyryev, L. Baum, K. Matsuda, B. Hemmerling, and J. M. Doyle, J. Phys. B **49**, 134002 (2016).

[47] O. Emile, R. Kaiser, C. Gerz, H. Wallis, A. Aspect, and C. Cohen-Tannoudji, J. Phys. II (France) **3**, 1709 (1993).

[48] B. Sheehy, S. Q. Shang, P. Van Der Straten, S. Hatamian, and H. Metcalf, Phys. Rev. Lett. **64**, 858 (1990).

[49] A. Aspect, J. Dalibard, A. Heidmann, C. Salomon, and C. Cohen-Tannoudji, Phys. Rev. Lett. **57**, 1688 (1986).

[50] S. Padua, C. Xie, R. Gupta, H. Batelaan, T. Bergeman, and H. Metcalf, Phys. Rev. Lett. **70**, 3217 (1993).

[51] M. Zeppenfeld, M. Motsch, P. W. H. Pinkse, and G. Rempe, Phys. Rev. A **80**, 041401 (2009).

[52] N. R. Hutzler, H.-I. Lu, and J. M. Doyle, Chem. Rev. **112**, 4803 (2012).

[53] I. Kozyryev, L. Baum, K. Matsuda, P. Olson, B. Hemmerling, and J. M. Doyle, New J. Phys. **17**, 045003 (2015).

[54] D. Fletcher, K. Jung, C. Scurlock, and T. Steimle, J. Chem. Phys. **98**, 1837 (1993).

[55] J. Nakagawa, R. F. Wormsbecher, and D. O. Harris, J. Mol. Spectrosc. **97**, 37 (1983).

[56] B. Hemmerling, G. K. Drayna, E. Chae, A. Ravi, and J. M. Doyle, New J. Phys. **16**, 063070 (2014).

[57] Y. Cunyun, *Tunable external cavity diode lasers* (World Scientific, Hackensack, NJ, 2004).

[58] D. J. Berkeland and M. G. Boshier, Phys. Rev. A **65**, 033413 (2002).

[59] G. Herzberg, *Molecular Spectra and Molecular Structure: Electronic Spectra and Electronic Structure of Polyatomic Molecules* (Van Nostrand, New York, 1966), Vol. 3.

[60] M. D. Oberlander, Ph.D. thesis, Ohio State University, 1995.

[61] M. D. Hoogerland, H. F. P. de Bie, H. C. W. Beijerinck, E. J. D. Vredenbregt, K. A. H. van Leeuwen, P. van der Straten, and H. J. Metcalf, Phys. Rev. A **54**, 3206 (1996).

[62] Phase space density is given by $\Omega = n\lambda_{\mathrm{dB},x}\lambda_{\mathrm{dB},y}\lambda_{\mathrm{dB},z}$, where n is the number density and $\lambda_{\mathrm{dB},i} = h/\sqrt{2\pi m k_B T_i}$ is the thermal de Broglie wavelength for molecules with mass m and temperature T. Ω is an important figure of merit for many experiments [18].

[63] We compare the ratio of the peak on-axis LIF signals in order to extract the number density ratio.

[64] B. Klöter, C. Weber, D. Haubrich, D. Meschede, and H. Metcalf, Phys. Rev. A **77**, 033402 (2008).

[65] J. Devlin and M. Tarbutt, New J. Phys. **18**, 123017 (2016).

[66] S. Chu, Rev. Mod. Phys. **70**, 685 (1998).

[67] A. Aspect, R. Kaiser, N. Vansteenkiste, and C. Westbrook, Phys. Scr. **T58**, 69 (1995).

[68] W. D. Phillips, Rev. Mod. Phys. **70**, 721 (1998).

[69] A. Aspect, Phys. Rep. **219**, 141 (1992).

[70] H. J. Metcalf and P. van der Straten, J. Opt. Soc. Am. B **20**, 887 (2003).

[71] C. Cohen-Tannoudji, Phys. Rep. **219**, 153 (1992).

[72] J. Dalibard and C. Cohen-Tannoudji, J. Opt. Soc. Am. B **6**, 2023 (1989).

[73] M. Hoogerland, H. Beijerinck, K. van Leeuwen, P. van der Straten, and H. Metcalf, Europhys. Lett. **19**, 669 (1992).

[74] B. Sheehy, S.-Q. Shang, P. Van Der Straten, and H. Metcalf, Chem. Phys. **145**, 317 (1990).

[75] M. Hoogerland, J. Driessen, E. Vredenbregt, H. Megens, M. Schuwer, H. Beijerinck, and K. Van Leeuwen, Appl. Phys. B **62**, 323 (1996).

[76] J. Söding, R. Grimm, Y. B. Ovchinnikov, P. Bouyer, and C. Salomon, Phys. Rev. Lett. **78**, 1420 (1997).

[77] M. Prentiss and A. Cable, Phys. Rev. Lett. **62**, 1354 (1989).

[78] R. Nicholls, Astrophys. J. Suppl. Ser. **47**, 279 (1981).

[79] C. Brazier, L. Ellingboe, S. Kinsey-Nielsen, and P. Bernath, J. Am. Chem. Soc. **108**, 2126 (1986).

[80] P. F. Bernath, Adv. Photochem. **23**, 1 (1997).

[81] I. Kozyryev, L. Baum, K. Matsuda, and J. M. Doyle, ChemPhysChem **17**, 3641 (2016).